

DECOMPRESSION THEORY: A DYNAMIC CRITICAL-VOLUME HYPOTHESIS

D. E. Yount and D. C. Hoffman

As emphasized by Hills (1,2), there are two basically different approaches to decompression optimization. The first is to devise a convenient calculational method and then modify it empirically until it is in reasonable agreement with the available data. The second is to develop a theoretical model from fundamental physical and physiological principles and then attempt to quantify its response to changes in exposure pressure. A key issue in either case is the identification of the proper decompression criterion.

The empirical approach is illustrated by the method of Haldane (3). The Haldane decompression criterion is expressed as a pressure ratio, which has been interpreted a posteriori as a supersaturation limit for the formation of bubbles whose mere presence is assumed to cause symptoms (4). Alternatively, the ratio could represent a critical volume of separated gas or a critical degree of embolism that the body can tolerate (5). This second possibility was mentioned already in Ref. 3; however, since it is not rigorously compatible with the assumptions of exponential gas exchange and of symmetric gas uptake and elimination, it cannot properly be regarded as a bona fide part of the Haldane scheme (1,2).

The theoretical approach is illustrated by the method of Hills (6), which is based on the principle of *phase-equilibration*. In Hills' regime, bubble formation is assumed to be so profuse in the relevant tissues that all gas in excess of equilibrium is "dumped" into the gas phase within a few minutes after a pressure reduction. If one further assumes that the volume of separated gas is critical, the result is not a pressure ratio but a *zero-supersaturation* criterion for decompression (1,2).

The physiological circumstances implicit in the Haldane method (4) represent the "best case" in the sense that little or no gas has come out of solution.

The circumstances envisioned by Hills (1,2) correspond to the "worst case" because the volume of separated gas is maximal. In addition, the pressure gradient for eliminating gas via the circulation, essentially the supersaturation P_{ss} , is maximal for Haldane and minimal for Hills.

Evidently, the best-case and worst-case calculational methods of Haldane and of Hills, founded respectively on no gas release and on complete phase equilibration, lie at opposite ends of the bubble formation or nucleation spectrum (2). The truth, we believe, lies somewhere in between. There is ample evidence that bubble formation does occur routinely in asymptomatic Haldanian decompressions (7), and there is also ample evidence that the total volume of released gas at the onset of mild decompression symptoms is much smaller than would be required by phase equilibration. Rubissow and Mackay (8), working with rats, have found that following initial decompressions, 2–10 bubbles with diameters of 2–5 μm are present per mm^3 in fatty tissue. This corresponds to a volume of gas released into bubbles, which is less than 10^{-5} of that still in solution. More recently, Hills (9) has estimated that 17% of the dissolved gas was released in guinea pigs decompressed from 4 atm abs to 2.21 atm abs, while 21% was released in going from 4 atm abs to 1 atm abs. The corresponding decreases in nitrogen washout rates were only 7 and 15%, respectively.

With the development of a detailed mathematical model describing bubble formation in aqueous media (10), it is now possible to quantify various degrees of nucleation and place any given dive profile at a more realistic position on the nucleation scale. The methods of Haldane and of Hills may then be regarded as limiting special cases of a more general decompression theory that should someday be applicable to the whole range of hyperbaric and hypobaric situations.

In the remainder of this paper, we report on our first attempts to calculate a comprehensive set of diving tables by applying nucleation theory. The computational algorithms are summarized in the next section, and results are discussed in the section that follows. A promising feature of the new tables is that they give sensible prescriptions for a wide range of diving situations, yet employ a small number of parameters and a single set of parameter values. All of the calculations reported here were carried out on an ordinary home computer (Radio Shack TRS-80 with 48K memory).

METHODS

In previous applications of our nucleation model to decompression sickness (11–13), we were dealing mainly with rudimentary pressure schedules in which the subjects were first saturated with gas at some elevated pressure P_1 and then supersaturated by reducing the pressure from P_1 to the final setting P_2 . The data in such experiments are most easily presented by plotting the combinations of supersaturation versus exposure pressure ($P_{ss} \approx P_1 - P_2$ versus P_1), which yield a given morbidity, for example, a 50% probability of

contracting decompression sickness. To describe these data, we assumed that lines of constant morbidity were also lines of constant bubble number N (11–13). The bubble number, in turn, was assumed to be equal to the number of spherical gas nuclei with initial radii r_0 larger than some minimum radius r_0^{\min} (10). This approach was remarkably successful, partly because the schedules involved were so simple—representing, as it were, a type of controlled experiment in which most of the variables in the problem were fixed.

Our naive assumption of constant nucleation or constant bubble number does not encompass the full range of conditions covered by modern diving tables. That is, it yields a set of tables which, though they may be very safe, do not track conventional tables in their global behavior and often require total ascent times that would generally be considered excessive by the commercial diving industry. Treating the conventional tables as valid experimental data, we have been forced to develop a more comprehensive decompression criterion.

The first step has been to replace *constant bubble number* with a *critical-volume hypothesis*, thereby assuming that signs or symptoms will appear whenever the total volume V accumulated in the gas phase exceeds some designated critical value V_{crit} . Although V_{crit} itself is fixed for all of our diving tables, gas is continuously entering and leaving the gas phase. In this sense, our decompression criterion is dynamic, rather than static as in other applications of the critical-volume point of view (14).

The idea that gas is continuously leaving the gas phase is suggested by our previous work (11–13), which seems to imply that there is a bubble number N_{safe} that can be tolerated indefinitely, regardless of the degree of supersaturation P_{ss} . From this, we deduce that the body must be able to dissipate free gas at a useful rate that is proportional both to N_{safe} and to P_{ss} . A possible rationale is provided by physiological studies demonstrating that so long as its capacity is not exceeded, the lung is able to continue functioning as a trap for venous bubbles (15).

Another implication of our present investigation is that in practical diving tables (and especially in surface-decompression procedures), the actual number of supercritical nuclei N_{actual} is allowed temporarily to exceed the number that can be tolerated indefinitely N_{safe} . This permits the volume of the gas phase to inflate at a rate that is proportional to $P_{\text{ss}} (N_{\text{actual}} - N_{\text{safe}})$. In our present formulation, the increase in gas-phase volume continues until P_{ss} is zero. At this point, usually long after the dive has ended, the net volume of released gas has reached its maximum value V_{max} , which must be less than V_{crit} if signs and symptoms of decompression sickness are to be avoided.

Our computation of a diving table begins with the specification of six nucleation parameters. These are the surface tension γ , the nuclear skin compression γ_C (10), the minimum initial radius r_0^{\min} (10), the pressure p^* at which the skins become impermeable to gas (10), the time constant τ_R for the regeneration of nuclei crushed in the initial compression (16), and a composite parameter λ , which is related to V_{crit} and determines, in effect, the amount by which the actual bubble number N_{actual} can exceed the safe bubble number N_{safe} .

N_{actual} is much larger than N_{safe} for short dives, but the two are nearly equal for dives of long duration.

From the given set of parameter values, the program calculates a preliminary estimate of P_{ss} that is just sufficient to probe the minimum initial radius $r_{\text{o}}^{\text{min}}$ and hence to produce a number of bubbles equal to N_{safe} . In the permeable region of the model, the nuclear radius $r_{\text{i}}^{\text{min}}$ following an increase in pressure from P_{o} to P_{i} can be obtained from the equation (10)

$$(1/r_{\text{i}}^{\text{min}}) = (1/r_{\text{o}}^{\text{min}}) + (P_{\text{i}} - P_{\text{o}})/2(\gamma_{\text{C}} - \gamma). \quad (1)$$

Regeneration of the nuclear radius is allowed to take place throughout the time t_{R} after P_{i} is reached. This is a complex statistical-mechanical process (16), which we have chosen to approximate via an exponential decay with the regeneration time constant τ_{R} :

$$r(t_{\text{R}}) = r_{\text{i}}^{\text{min}} + (r_{\text{o}}^{\text{min}} - r_{\text{i}}^{\text{min}})[1 - \exp(-t_{\text{R}}/\tau_{\text{R}})]. \quad (2)$$

The supersaturation of P_{ss}^{o} that is just sufficient to probe $r_{\text{o}}^{\text{min}}$ is then found from (10)

$$P_{\text{ss}}^{\text{o}} = 2(\gamma/\gamma_{\text{C}})(\gamma_{\text{C}} - \gamma)/r(t_{\text{R}}). \quad (3)$$

Holding P_{ss}^{o} fixed, the program next calculates a decompression profile and the total decompression time t_{D} . From t_{D} and the constant

$$\beta_{\text{o}} = 2(\gamma_{\text{C}} - \gamma)/r_{\text{o}}^{\text{min}}, \quad (4)$$

a new value $P_{\text{ss}}^{\text{new}}$ is obtained which will probe a new initial radius $r_{\text{o}}^{\text{new}}$ that is smaller than $r_{\text{o}}^{\text{min}}$ and hence will result in a number of bubbles that is larger than N_{safe} .

In principle, the revised bubble number $N(r_{\text{o}}^{\text{new}})$ can be found by assuming that the integral radial size distribution of spherical gas nuclei in vivo is a decaying exponential (16,17),

$$N(r_{\text{o}}^{\text{new}}) = N_{\text{o}} \exp(-\beta_{\text{o}} S r_{\text{o}}^{\text{new}}/2kT), \quad (5)$$

where S is the skin area occupied by one surfactant molecule in situ, k is the Boltzmann constant, and T is the temperature. In practice, however, the absolute bubble number N and the net gas volume V are not explicitly determined since the arbitrary normalization N_{o} of the nuclear size distribution cancels out.

After several pages of mathematical manipulation, we have derived a simple formula for $P_{\text{ss}}^{\text{new}}$ that takes into account the critical volume V_{crit} , the exponential radial distribution $N(r_{\text{o}}^{\text{new}})$, and the inflation of the gas phase—essentially the time integral of P_{ss} ($N_{\text{actual}} - N_{\text{safe}}$). The result, which must be recalculated for each tissue half time H , is

$$P_{\text{ss}}^{\text{new}} = P_{\text{ss}}^{\text{o}} \{1 + \lambda/[(\beta_{\text{o}} + P_{\text{i}} - P_{\text{o}})(t_{\text{D}} + H/0.693)]\}, \quad (6)$$

where S , k , and T have been absorbed into the composite *critical-volume* parameter λ . Using the respective values of $P_{\text{ss}}^{\text{new}}$ for each ‘‘tissue compartment,’’ the program determines a more severe decompression profile, which

will yield updated values of t_D and P_{ss}^{new} . After several iterations, t_D and P_{ss}^{new} converge, implying that V_{max} now differs from V_{crit} by an acceptably small amount.

The uptake and elimination of inert gas by the body is assumed to be exponential, as in conventional tables (18). Water vapor pressure and the dissolved partial pressures of oxygen and carbon dioxide are calculated in the manner described in Ref. 19. The net contribution of these “active” gases is nearly constant at 102 mmHg for inspired oxygen pressures up to about 2 atm abs. This limit is not reached for air decompression tables at ambient pressures below about 10 atm abs. The half times H for the various tissue compartments are 1, 2, 5, 10, 20, 40, 80, 120, 160, 240, 320, 400, 480, 560, and 720 min. The onset of impermeability, $p^* = 9.2$ atm abs, is high enough so that nearly all of our air decompression tables lie in the “permeable” or “linear” region of our nucleation model (10).

Because the model predictions depend only upon the ratios γ/γ_C and $2\gamma/r_o^{min}$, the value of γ is essentially arbitrary (10,13). To be definite, however, we have set $\gamma = 17.9$ dyn/cm (20). With this choice, the values of the remaining four parameters are $\gamma_C = 257$ dyn/cm, $r_o^{min} = 0.775$ μ m, $\tau_R = 20,160$ min, and $\lambda = 5000$ fsw/min. These were found by requiring that the total decompression times in our tables resemble those in the TEKTITE saturation dive (21) and in the U.S. Navy (22) and Royal Naval Physiological Laboratory (23) manuals. In other words, all of the results reported in this paper were obtained by optimizing the values of only four nucleation parameters, γ_C , r_o^{min} , τ_R , and λ .

Depths and pressures are usually given in feet of sea water (33 fsw = 10 msw = 1 atm = 2 atm abs, etc.) for convenience in making comparisons with the TEKTITE, USN, and RNPL reference schedules. For similar total decompression times, the set of tables generated in this study is expected to yield smaller total bubble volumes and therefore to be safer. None of the tables has as yet been tested on either animal or human subjects.

RESULTS

In this section, the salient features of a number of diving tables using air as the breathing mixture are compared. The VPM and USN (22) profiles for an *exceptional exposure* involving greater than normal risk are shown in Fig. 1. In both cases, the descent and ascent rates are 60 fsw/min, and the 3.33 min required to reach 200 fsw is counted as part of the 60-min bottom time. The total decompression times are similar, the important difference being the deeper *first stop* of the VPM table, 130 fsw versus 60 fsw for USN. This is a persistent feature of the literally hundreds of comparisons we have made of VPM tables with a variety of conventional tables now in use. Our calculations indicate that the longer “first-pull” of these conventional tables results in a larger supersaturation P_{ss} , in a larger bubble number N , and ultimately in a larger maximum volume of released gas V_{max} .

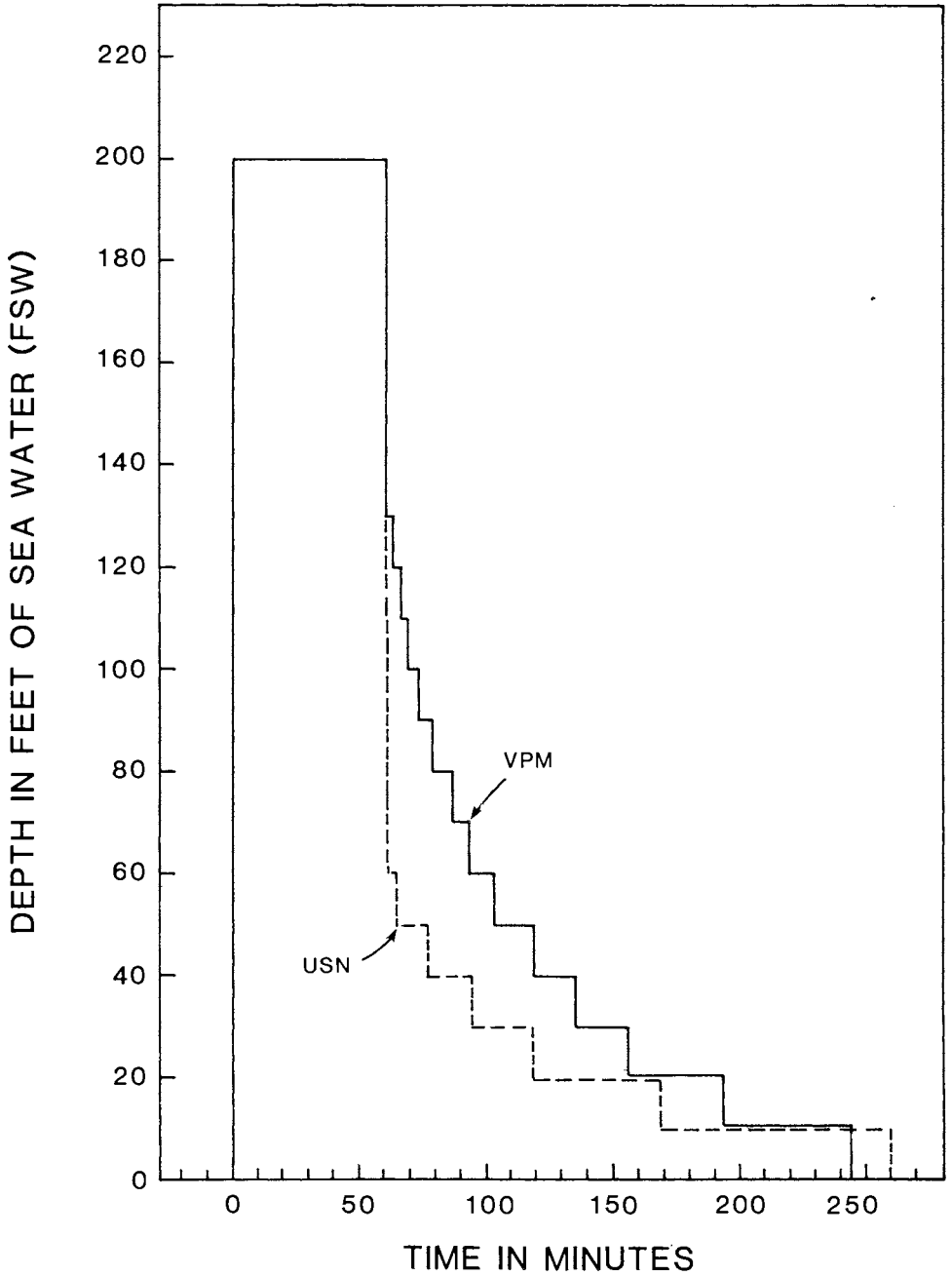


Fig. 1. Varying-permeability model (VPM) and U.S. Navy (USN) decompression profiles for a 60-min dive to 200 fsw. The longer "first-pull" of conventional tables results in a larger supersaturation P_{ss} , a larger bubble number N , and ultimately in a larger maximum volume of released gas V_{max} .

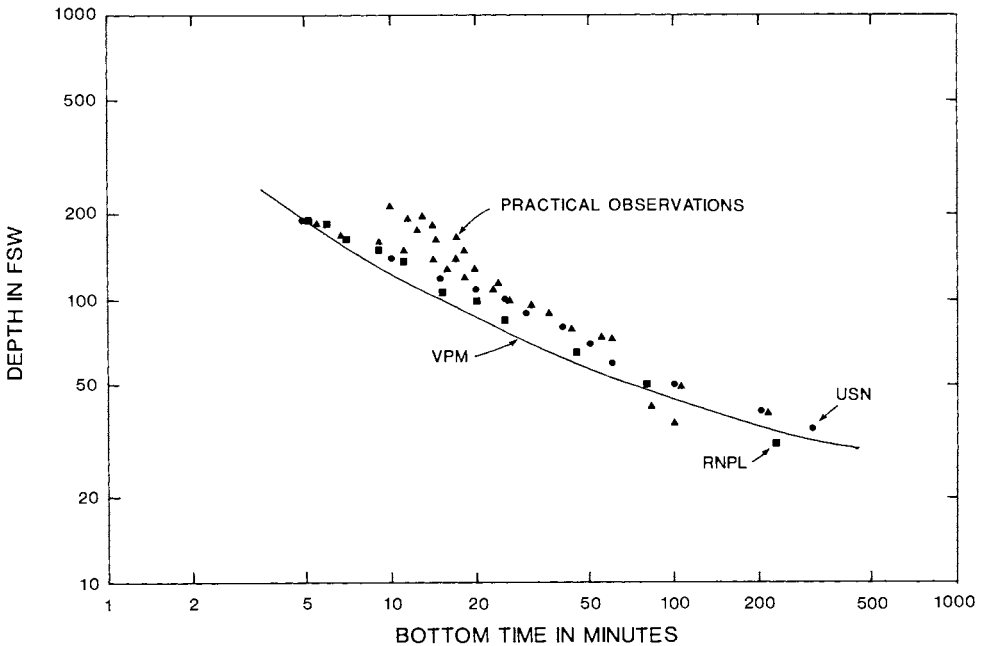


Fig. 2. Comparison of varying-permeability model (VPM), U.S. Navy (USN), and Royal Naval Physiological Laboratory (RNPL) *no-stop* decompressions with various practical observations, i.e., combinations of depth and bottom time that yielded no symptoms or only the mildest symptoms. The VPM curve lies just below the USN and RNPL recommendations at all but one RNPL point and therefore serves as a safe, tight, and useful lower bound.

Figure 2 compares VPM, USN (22), and RNPL (23) *no-stop* decompressions, along with various “practical observations” compiled by Leitch and Barnard (24). Although there are some differences in this plot in the rates of descent and ascent and in the exposure conditions (24), the absence of prolonged decompression stages makes this type of “data” nearly independent of the overall surfacing strategy. The VPM curve lies just below the USN and RNPL recommendations at all but one RNPL point (230 min at 33 fsw), and over the entire range, it serves as a safe, tight, and therefore useful lower bound. The fact that the VPM curve is a bit low in this case reflects the general conservatism of the tables we have prepared. A bolder, more aggressive set of tables could, of course, be computed by simply adjusting the values of the nucleation parameters.

Total ascent times for VPM, USN (22), and RNPL (23) are plotted as a function of the bottom time at 200 fsw in Fig. 3. The VPM curve lies close to the USN points for bottom times that extend all the way from 5 to 360 min. The large difference in USN and RNPL total ascent times (often more than a factor of 2) illustrates the wide divergence in opinion that still exists, even among highly respected investigators in the diving field.

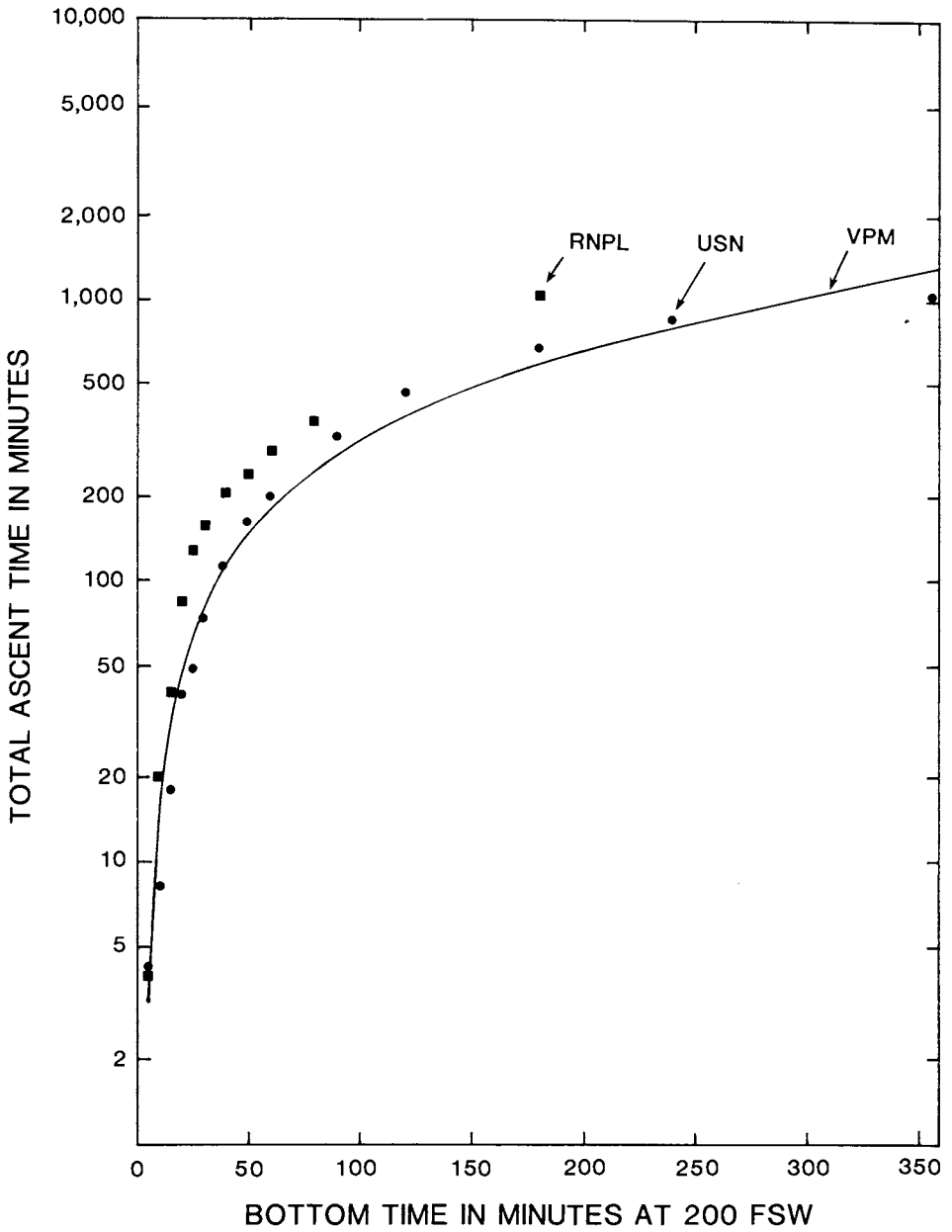


Fig. 3. Total ascent times versus bottom times at 200 fsw for VPM, USN, and RNPL decompression tables. The total ascent times for USN and RNPL often differ by more than a factor of 2.

One very practical reason for attempting to optimize decompression procedures from first principles is the hope that if a correct global theory can someday be formulated, it will then be possible to relate and describe the whole range of decompression experience with a small number of equations and parameter values. Instead of “titrating” a handful of “volunteers” to develop a new table or determine a new M -value (22), a method which necessarily has limited statistical accuracy, one will be able to use an already calibrated theory to interpolate or extrapolate, thereby bringing to bear the full statistical weight of a much larger data base. This idea is illustrated in Fig. 4, which summarizes total ascent times versus bottom times for VPM decompressions from air dives to 60, 100, 200, and 300 fsw.

As a second illustration of the global approach, Fig. 5 connects the no-stop decompressions in Fig. 2 with the 14-day, 100-fsw TEKTITE saturation dive (21). The latter has been used by humans without incident. However, the close agreement apparent in this graph is partly fortuitous because the TEKTITE stops were 5 rather than 10 fsw apart, and the breathing gas was a normoxic oxygen-nitrogen mixture rather than air. In addition, both air and pure oxygen were breathed during various stages of the TEKTITE decompression. A more precise comparison is given in Table I, where the VPM schedule was calculated for a 14-day exposure to the 126-fsw equivalent air depth of the TEKTITE dive.

By replacing our earlier assumption of constant bubble number with a dynamic critical-volume hypothesis, we have succeeded in preparing a comprehensive set of air diving tables which, though untested, appear in all respects to be quite reasonable. It should not be forgotten, however, that the constant-bubble-number criterion did work well in those rudimentary cases in which it was first applied (11–13). This raises the question of whether our new and different criterion can also describe these special situations. The answer is affirmative, suggesting that our tables obey a kind of *correspondence principle* in which *critical volume* becomes equivalent to *constant bubble number* in the limit of a nucleation-dominated regime, i.e., a regime in which N_{actual} approaches N_{safe} and the allowed supersaturation P_{ss} is determined directly by $r_{\text{o}}^{\text{min}}$.

An illustration of the critical-volume \leftrightarrow critical-nucleation correspondence for humans is provided by Fig. 6. The rudimentary cases referred to in this figure, in the previous paragraph, and also at the beginning of the METHODS section are those in which the subjects are first saturated with gas at some elevated pressure P_1 and then supersaturated by reducing the pressure from P_1 to the final setting P_2 . In experiments with human subjects, $P_1 - P_2$ is usually defined as the greatest pressure reduction that can be sustained without the onset of decompression sickness. To simulate this condition with our tables, we have selected dives with bottom times of 720 min and have taken P_2 to be the depth of the first decompression stop. This provides a reasonable approximation to a single-step decompression in the nucleation-dominated regime because, in this limit, the rate at which gas is permitted to come out of solution is just slightly larger than that which the body can dissipate and therefore tolerate indefinitely.

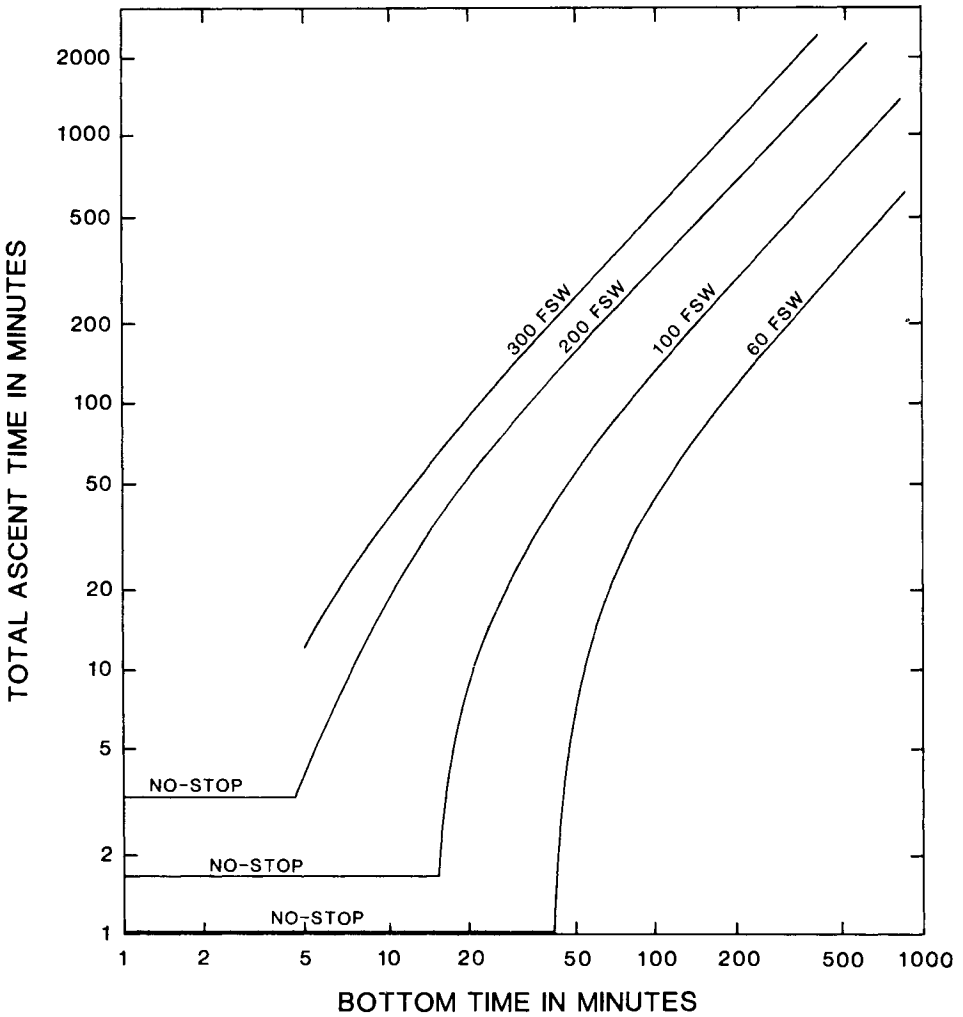


Fig. 4. Total ascent times versus bottom times for VPM at depths of 60, 100, 200, and 300 fsw. This figure and the one which follows illustrate how a large range of decompression experience can be described by a global theory using a small number of equations and parameter values.

In the permeable region of our nucleation model ($P_1 < p^* = 9.2$ atm abs), this procedure yields a linear relationship,

$$P_1 = 1.372 P_2 + 0.335 \text{ atm abs}, \tag{7}$$

which has a correlation coefficient of better than 0.999 for the eight combinations of P_1 and P_2 which were used. Similar expressions,

$$P_1 = 1.375 P_2 + 0.52 \text{ atm abs} \tag{8}$$

and

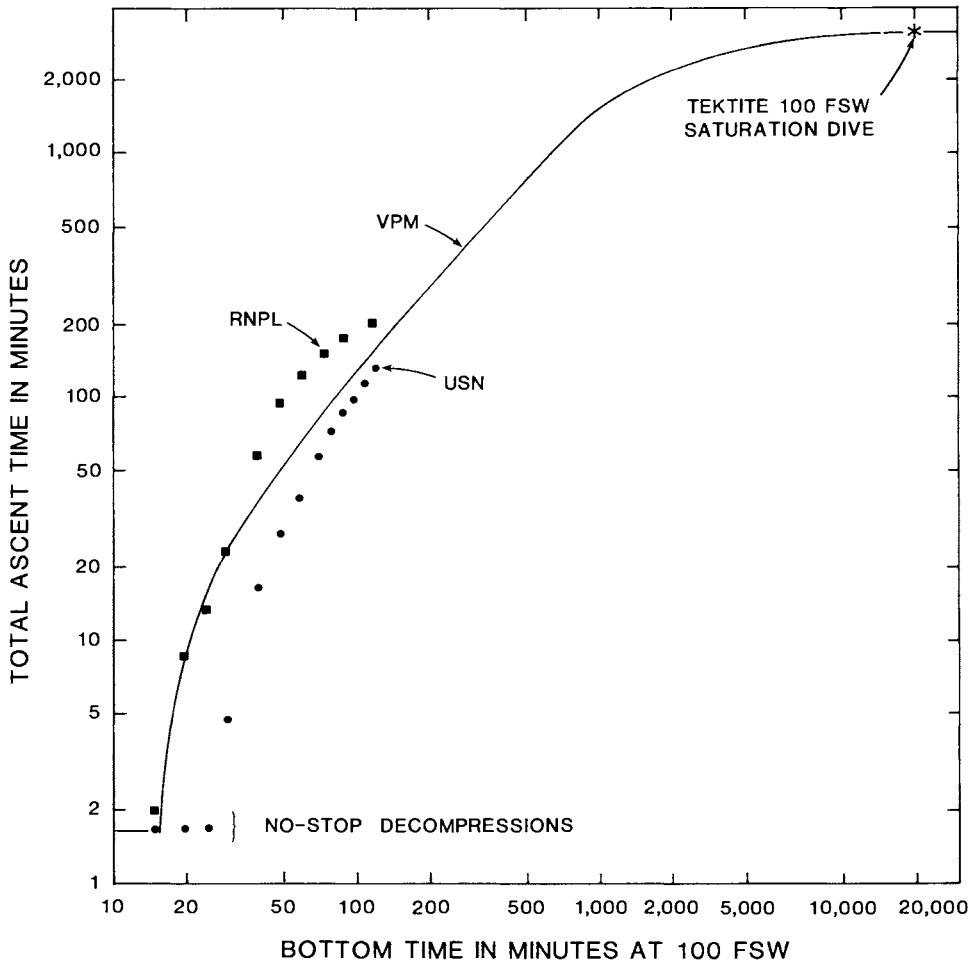


Fig. 5. Total ascent times versus bottom times at 100 fsw for VPM, USN, RNPL, and TEKTITE decompression tables. All of the VPM schedules reported in this paper were computed with the same values of the four adjustable nucleation parameters γ_c , r_0^{\min} , τ_R , and λ .

$$P_1 = 1.366 P_2 + 0.56 \text{ atm abs,} \quad (9)$$

have been extracted by Hennessy and Hempleman (14) from, respectively, the USN and RNPL tables. As can be seen in Fig. 6, the *three straight lines* are nearly parallel, and VPM is 0.1 to 0.2 atm lower than USN and RNPL. The fact that these lines are similar to the isopleths of constant bubble number presented for the permeable region in Refs. 11, 12, and 13 verifies the above mentioned correspondence for this rudimentary case. The *no-stop threshold*, $P_1 = 1.87 \text{ atm abs}$ and $P_1 - P_2 = 0.87 \text{ atm}$, was obtained by averaging the values of $P_1 = 1.90 \text{ atm abs}$, $P_1 - P_2 = 0.90 \text{ atm}$ measured by Hempleman

TABLE I
 Comparison of the 14-day, 100-fsw TEKTITE Decompression
 Table with the Equivalent VPM Schedule

Depth (fsw)	Time at Stop (min) TEKTITE	Time at Stop (min) VPM
100-90	10 air	
90	60 air	
85	90 air	21 air
80	100 air	157 air
75	110 air	163 air
70	120 air	168 air
65	360 air	175 air
60	140 air	181 air
55	160 air	188 air
50	160 air	196 air
45	10 oxy	204 air
	150 air	
40	130 air	213 air
35	20 oxy	222 air
	150 air	
30	360 air	234 air
25	30 oxy	246 air
	150 air	
20	150 air	259 air
15	50 oxy	273 air
	120 air	
10	160 air	291 air
5	60 oxy	309 air
	110 air	
TOTAL	2960 (+ 170 oxy) (3130)	3502

(25) with those of $P_1 = 1.83$ atm abs, $P_1 - P_2 = 0.83$ atm found by Kidd, Stubbs, and Weaver (26). The VPM result is $P_1 = 1.71$ atm abs, $P_1 - P_2 = 0.71$ atm. The *altitude bends threshold* plotted in Fig. 6, namely, $P_1 = 1.00$ atm abs, $P_1 - P_2 = 1.00 - 0.40 = 0.60$ atm, was calculated from the value of $P_2 = 7550$ m = 307 mmHg = 0.40 atm abs determined by Gray (27). The VPM limit of $P_1 = 1.00$ atm abs, $P_1 - P_2 = 0.52$ atm is again slightly lower. The extrapolations of the lines for USN and RNPL (14) are both slightly higher than the experimental no-stop and altitude bends thresholds plotted in this figure.

DISCUSSION

We are aware that this investigation, though promising, can be criticized on a number of grounds. The most serious, we believe, is the fact that none

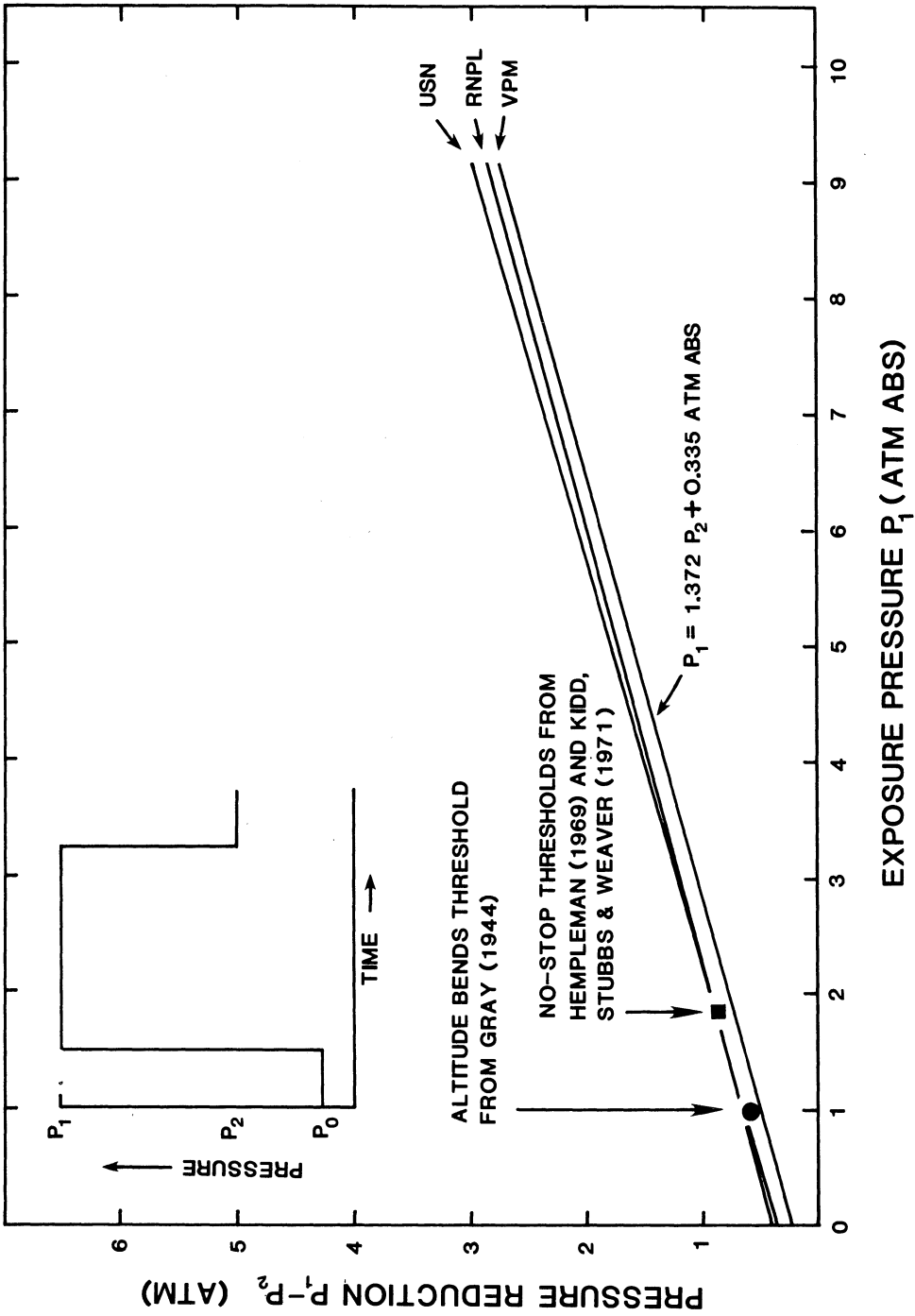


Fig. 6. Allowed pressure reduction $P_1 - P_2$ versus exposure pressure P_1 for USN, RNPL, and VPM air diving tables. In the limit of a nucleation-dominated regime, lines of constant critical volume are also isopleths of constant bubble number.

of our diving tables have been tested. Unfortunately, we have neither the resources nor the support to sustain such an effort. Our immediate goal, therefore, was not to produce an operational set of diving tables but instead to determine whether a reasonable and comprehensive set of such tables could be computed from our nucleation model using a modest number of assumptions, equations, and parameter values. The answer, quite obviously, is yes.

Our operational definition of *reasonable and comprehensive* is: *similar, both in scope and in total decompression time, to other tables now in use*. A possible criticism here is that some of the reference tables are not very safe, and we may be trying too hard to match them, for example, by abandoning our original goal of zero or constant (but physiologically insignificant) bubble number. Alternatively, we may be losing a chance to shorten decompression obligations and improve diving efficiency. This is a matter of judgment in which we have decided to begin by accepting the whole range of diving experience, including conventional tables, as useful experimental data. Greater safety and/or efficiency may then become feasible both through an improved decompression strategy, as in Fig. 1, and through the unification and “smoothing” which result when a global theory is applied to a broad data sample. What is not a matter of judgment, but an early conclusion of this investigation, is the fact that any set of tables based on zero or constant bubble number is likely to be very different in global behavior from other tables now in use.

Another criticism is that we have said very little about the physiological processes that presumably underlie our mathematical equations. We take oxygen and carbon-dioxide into account and assume a reasonable range of tissue half times, but many other details are overlooked. We make no distinction, for example, between “fatty, loose tissue” and “watery, tight tissue” (14), nor do we state explicitly where the bubbles form or how they grow, multiply, or are transported. Finally, we say nothing about such factors as solubility, diffusion versus perfusion, tissue-deformation pressure, or tissue-specific differences in surface tension. Our response to criticisms of this type is that most of the omitted processes are poorly understood, and their inclusion at this stage would serve only to complicate the model and increase the number of undetermined parameters.

As a by-product of this investigation, we have gained a better understanding of practical decompression tables now in use. We believe, for example, that profuse bubble formation is permitted by such tables, particularly during dives of short duration. Meanwhile, the number of primary bubbles, i.e., bubbles formed directly from nuclei rather than from other bubbles (28), is allowed to vary widely. The common assumption (3,5,6,14) that the volume of released gas is critical seems still to be viable providing allowance is made for the body’s ability to dissipate free gas at a useful rate (15). Since gas is continuously entering or leaving the gas phase, optimal decompression is defined by a *dynamic critical-volume hypothesis* requiring that the *net* volume of free gas be always less than the threshold value V_{crit} .

Acknowledgments

We are especially grateful to Gilbert Grenié of the École Centrale des Arts et Manufactures, Chatenay-Malabry, France, who visited the University of Hawaii for several months in 1980 and played a key role in the initial stages of this investigation. Other visitors from the École Centrale who have participated in this program are Bernard Rémy in 1981, Gildas Herjean in 1982, and Philippe Mazas in 1983. We also wish to thank our colleagues Ed Beckman, Claude Harvey, Jon Pegg, and Birch Porter for useful suggestions and comments. This work, carried out under "The Physics of Gas Bubbles: Medical Applications" Project (HP/R-4), is a result of research sponsored in part by the University of Hawaii Sea Grant College Program under Institutional Grant Number NA81AA-D-00070 from NOAA Office of Sea Grant, U.S. Department of Commerce.

References

1. Hills BA, Vital issues in computing decompression schedules from fundamentals. I. Critical supersaturation versus phase equilibration. In *J Biometeor* 1970;14:111-131.
2. Hills BA. Zero-supersaturation approach to decompression optimization. In: Hong SK, ed. *International symposium on man in the sea*. Bethesda: Undersea Medical Society, Inc., 1975:179-189.
3. Boycott AE, Damant GCC, Haldane JS. The prevention of compressed air illness. *J Hyg (Camb)* 1908;8:342-443.
4. Workman RD. Calculation of decompression schedules for nitrogen-oxygen and helium-oxygen dives. Washington, DC: U.S. Navy Experimental Diving Unit, 1965. (NEDU report no. 6-65)
5. Behnke AR. Decompression sickness following exposure to high pressures. In: Fulton JF, ed. *Decompression sickness*. Philadelphia: W. B. Saunders & Co., 1951:53-89.
6. Hills BA. A thermodynamic and kinetic approach to decompression sickness. Ph.D. Thesis. Adelaide: Library Board of South Australia, 1966.
7. Spencer, MP, Campbell SD. Development of bubbles in venous and arterial blood during hyperbaric decompression. *Bull Mason Clinic* 1968;22:26-32.
8. Rubissow GJ, Mackay RS. Decompression study and control using ultrasonics. *Aerosp Med* 1974;45:473-478.
9. Hills BA. Effect of decompression per se on nitrogen elimination. *J Appl Physiol: Respir Environ Exercise Physiol* 1978;45:916-921.
10. Yount DE. Skins of varying permeability: a stabilization mechanism for gas cavitation nuclei. *J Acoust Soc Am* 1979;65:1429-1439.
11. Yount DE. Responses to the twelve assumptions presently used for calculating decompression schedules. The Seventeenth Undersea Medical Society Workshop, Decompression theory. UMS Publ. No. 29WS(DT) 6-25-80. Bethesda: Undersea Medical Society, Inc., 1978:143-160.
12. Yount DE. Application of a bubble formation model to decompression sickness in rats and humans. *Aviat Space Environ Med* 1979;50:44-50.
13. Yount DE. Application of a bubble formation model to decompression sickness in fingerling salmon. *Undersea Biomed Res* 1981;8:199-208.
14. Hennessy TR, Hempleman HV. An examination of the critical released gas volume concept of decompression sickness. *Proc R Soc Lond Biol* 1977;197:299-313.
15. Butler BD, Hills BA. The lung as a filter for microbubbles. *J Appl Physiol: Respir Environ Exercise Physiol* 1979;47:537-543.
16. Yount DE. On the evolution, generation, and regeneration of gas cavitation nuclei. *J Acoust Soc Am* 1982;71:1473-1481.
17. Yount DE, Gillary EW, Hoffman, DC. Microscopic study of bubble formation nuclei. In: Bachrach AJ, Matzen MM, eds. *Underwater physiology VIII. Proceedings of the eighth symposium on underwater physiology*. Bethesda, Undersea Medical Society, Inc., 1984:119-130.
18. Yount DE, Strauss RH. Decompression sickness. *Am Sci* 1977;65:598-604.
19. Yount DE, Lally DA. On the use of oxygen to facilitate decompression. *Aviat Space Environ Med* 1980;51:544-550.

20. Davson H. A textbook of general physiology. London: Churchill, 1964:185.
21. Beckman EL, Smith EM. TEKTITE II: medical supervision of the scientists in the sea. *Texas Reports on Biol and Med* 1972;30:155-169.
22. U.S. Navy diving manual (NAVSHIPS 0994-001-9010), U.S. Navy Department. Washington: U.S. Government Printing Office, 1970.
23. Air diving tables. Royal Naval Physiological Laboratory, Alverstoke, Hants. London: Her Majesty's Stationary Office, 1968.
24. Leitch DR, Barnard EEP. Observations on no-stop and repetitive air and oxynitrogen diving. *Undersea Biomed Res* 1982;9:113-129.
25. Hempleman HV. British decompression theory and practice. In: Bennett PB, Elliott DH, eds. *The physiology and medicine of diving and compressed air work*. Baltimore: Williams & Wilkins, 1969:331-347.
26. Kidd DJ, Stubbs RA, Weaver RS. Comparative approaches to prophylactic decompression. In: Lambertsen CJ, ed. *Proceedings of the fourth symposium on underwater physiology*. New York: Academic Press, 1971:167-177.
27. Gray JS. Aeroembolism induced by exercise in cadets at 23,000 feet. Washington, DC: UA Natl Res Council, 1944. (Comm Aviat Med report 260)
28. Yount DE. Multiple inert-gas bubble disease: a review of the theory. Twenty-second ONR/UMS workshop on isobaric inert gas counterdiffusion. Bethesda: Undersea Medical Society 1982;90-125.